Journal of Radioanalytical and Nuclear Chemistry (2026) 335:1215–1227
https://doi.org/10.1007/s10967-026-10734-1

Application of gamma irradiation for the decontamination of historical glass plate photographic negatives

Maria Luiza E. Nagai[1] · Elizabeth S. R. Somessari[1] · Tatiana A. Reis[2] · Pablo A. S. Vasquez[1]

Received: 29 April 2025 / Accepted: 7 January 2026 / Published online: 3 February 2026
© The Author(s) 2026

Abstract
Ionizing radiation is an effective method for fungal decontamination of photographic heritage materials; however, its application to glass plate negatives may induce optical darkening due to radiation-induced defects in the glass matrix. This study investigates the influence of temperature during gamma irradiation and the potential of UVB light exposure as a non-thermal bleaching strategy. Historical glass plate negatives were irradiated at 6 kGy under room temperature and dry-ice cooling, while common soda–lime–silica glass samples were used as analogues to quantify optical changes. Low-temperature processing mitigated color alterations without affecting decontamination efficacy, whereas UVB exposure promoted partial recovery of transparency in a dose-dependent manner. The combined approach offers a viable strategy for balancing biocidal effectiveness and optical preservation in glass-based photographic heritage.

Keywords Glass plate photographic negatives · Fungal contamination · Gamma irradiation · Ionizing radiation disinfection · Cultural heritage preservation

Introduction

Historical glass plate photographic negatives constitute important documentary artifacts, preserving visual records between the mid-19th and early 20th centuries. These materials are composite systems, consisting of a glass substrate coated with a light-sensitive photographic emulsion based on silver halides dispersed in either collodion, or gelatin, depending on the period of use [1]. While the glass support provides rigidity and dimensional stability, the organic emulsion is highly sensitive to environmental fluctuations, pollutants, and fungal activity. Consequently, glass plate negatives often exhibit degradation phenomena such as silver oxidation, image fading, gelatin swelling, cracking and biological colonization, especially under high humidity storage conditions. [2–4]. Fungal contamination is one of the most critical risks for photographic emulsions, as hyphae can penetrate and metabolize the gelatin layer, releasing hydrolytic enzymes that cause irreversible staining, softening, and loss of image information. Ionizing radiation has been explored as a decontamination method due to its biocidal effect, achieved within the 8 ± 2 kGy dose range recommended for mold, ensuring both microbiological safety and the preservation of the material [5–9]. However, the application of ionizing radiation to glass-based heritage materials must consider the formation of radiation-induced defects within the glass matrix. Gamma photons can generate color centers through the creation and trapping of electronic defects, resulting in optical darkening, increase absorbance in the visible region, and loss of image contrast. These effects depend on factors such absorbed dose, glass composition, and temperature during irradiation. Conventional methods to recover transparency in irradiated glass, such as heat treatments at temperatures starting from 100 °C [10–12], are unsuitable for glass negatives, given the heat sensitivity of photographic emulsion. Previous studies have investigated the use of light radiation, such as sunlight and mercury lamp, on irradiated glass materials, suggesting a potential bleaching effect [13–15]. In this study, UVB light exposure was chosen as bleaching treatment due to its energy being sufficient to release positive or negative charges trapped in the glass matrix which are responsible to

✉ Maria Luiza E. Nagai
malunagai@usp.br

[1] Nuclear and Energy Research Institute, Ave. Prof. Lineu Prestes, 2242, São Paulo 05508-000, Brazil

[2] Institute of Biomedical Sciences, Ave. Prof. Lineu Prestes, 2415, Sao Paulo 05508-000, Brazil

activate color centers, and thus promoting the restoration of transparency in the glass [16].

The use of low temperatures during ionizing radiation processing has demonstrated a protective role on biological and polymeric materials, mitigating the adverse effects of irradiation [17–21]. This protective effect, when applied using dry ice temperatures, may also benefit the irradiation of glassy materials. Additionally, the reduced mobility of crystalline defects at low temperatures can hinder their immediate recombination, thereby decreasing the formation or delaying the development of color centers. The slowdown of radiation-induced chemical reactions at low temperatures can help minimize undesirable side effects, such as glass darkening. However, previous studies have also suggested that cooling during irradiation could modify the sensitivity of microorganisms and other biological contaminants, requiring an increase in the dose needed to achieve complete decontamination, since reducing the temperature could attenuate the biocidal effect of irradiation [17, 22, 23]. For this reason, it was essential in the present study to evaluate whether the standard disinfection dose would remain effective under low temperature irradiation processing.

Despite the growing interest in radiation-based conservation strategies, few studies have examined the combined effects of irradiation parameters and post-treatment recovery on historical glass plate negatives. In particular, the influence of reduced temperatures during irradiation, which may suppress defect formation through limited atomic mobility, remains insufficiently explored in the context of photographic materials. Moreover, there is limited information on the applicability of controlled light exposure as a non-thermal approach to reverse radiation-induced optical changes. In light of these gaps, the present study aims to establish an innovative and alternative methodology for the treatment of glass plate photographic negatives contaminated by fungi, employing ionizing radiation processing without compromising their original characteristics. The goal is to contribute to the sustainable conservation of these unique records, ensuring their long-term preservation as vital elements of cultural memory. This study investigates the influence of temperature during ionizing radiation processing on historical glass plate negatives. Historical samples were exposed to γ-ray doses of 6 kGy, selected within the effective fungicidal range [5, 24, 25], under two temperature conditions: room temperature (RT) and dry ice (DI) cooling. Radiosensitivity was assessed in both temperature conditions through microbiological analysis. In addition to the historical materials, common glass samples were included as experimental controls. These samples were used to systematically investigate radiation-induced optical changes, particularly the formation of color centers and their evolution under different conditions. Since historical negatives are unique artifacts and cannot be damaged or subjected to destructive analytical procedures, common glass samples functioned as non-historical analogues, enabling controlled evaluation of UV-Vis absorbed changes, colorimetric shifts (ΔE) after irradiation at different doses, the effect of temperature during irradiation (RT vs DI) and kinetics of decay and UVB-induced bleaching. These control samples allowed isolation of the effects of radiation on the glass substrate itself, independent of the photographic emulsion, thus providing essential baseline data for interpreting changes observed in the historical negatives. Furthermore, the study proposes a new methodology for bleaching glass plate negatives that have undergone darkening as a result of the irradiation-based decontamination process. The results provide new insights into the safe and effective use of ionizing radiation for the conservation of glass-based photographic heritage.

Experimental

Sample description

Four glass plate photographic negatives, measuring 9 x 6.5 cm and 2 mm in thickness, were selected for this study from historical collections (Fig. 1). The samples were named according to their origin. The glass plate negatives selected from Cida Rivelli collection were designated by the initials CR (CR1, CR2 and CR3), while the copy from the Zoology Museum of the University of São Paulo was identified as MZ. No cleaning or surface intervention was performed to ensure that the biological load, optical properties, and physical features reflected authentic historical state of each object. These glass negatives exhibited signs of photographic emulsion oxidation, stains indicative of fungal contamination, and emulsion loss along the edges. In addition to the historical materials, the common glass samples, used for preliminary and comparative tests, were named CG. These glass pieces were obtained from contemporary photo frames and cut into standardized dimensions of 3 x 1 cm and 2 mm in thickness. These glass samples allowed isolation of the

Fig. 1 Samples of common glass (CG) and glass plate photographic negatives (CR1, CR2, CR3 and MZ) selected for study

effects of radiation on the glass substrate itself, independent of the photographic emulsion, thus providing essential baseline data for interpreting changes observed in the historical negatives.

Energy dispersive X-ray spectroscopy (EDS)

Qualitative elemental analyses of both the common glass (CG) samples and the historical photographic glass plate negatives were performed using energy dispersive X-ray spectroscopy (EDS) to identify the base glass type of the samples. Measurements were conducted with a Shimadzu EDX-720 spectrometer. This technique enabled the identification of the major and minor elements present in the glass matrices, contributing to the characterization and comparison of the materials used in the study. The detection limits of the EDX-720 system restrict measurable elements to those with atomic numbers between sodium (Na) and uranium (U). All measurements were carried out under atmospheric conditions, and the analyses focused exclusively on qualitative elemental identification.

Fourier transform infrared spectroscopy (FTIR-ATR)

To ensure the safe and effective application of gamma radiation treatment to fungal-contaminated glass photographic negatives, it was necessary to identify the constituent materials of the samples, with emphasis on characterizing the type of the photographic emulsion. This analytical step is essential, since different types of emulsions found in historical glass plate negative, such as those based on collodion or gelatin, have distinct chemical compositions that directly influence their response to ionizing radiation. Fourier transform infrared absorption spectra were obtained using an Agilent Cary 630 FTIR spectrometer equipped with an Attenuated Total Reflectance (ATR) module. FTIR-ATR spectra were acquired using a diamond ATR crystal. The spectra were recorded using Agilent MicroLab software, with automatic baseline correction and atmospheric compensation to spectral spectral resolution of 2 cm^{-1} and 128 accumulations per spectrum, in the spectral range of 4000 to 400 cm^{-1}.

Irradiation process by gamma rays

The samples were exposed to gamma radiation at the Multipurpose Co-60 Gamma Irradiation Facility of the Nuclear and Energy Research Institute – IPEN-CNEN/SP, Brazil, located on the University of São Paulo campus. The facility's current activity is approximately 13.0 PBq (350 kCi). To evaluate the formation and evolution of radiation-induced defects, the common glass samples (CG) were irradiated with gamma radiation at absorbed doses of 2, 6, 10, 15, and 25 kGy, at a dose rate of 1 $kGy{\cdot}h^{-1}$, divided in both temperature conditions of room temperature (RT) and with dry ice (DI). These doses were selected to cover both the typical decontamination range (6–8 kGy) and higher values relevant for studying defect kinetics, spectral signatures, and bleaching behavior. The use of multiple dose levels allowed detailed assessment of dose-dependent changes in absorbance, colorimetric parameters, and UVB-induced recovery. For glass negatives samples CR1, CR2, CR3 and MZ, the absorbed dose of 6 kGy applied at a dose rate of 1 $kGy.h^{-1}$ was selected because it falls within the minimum values in the internationally recommended 8 ± 2 kGy range for fungal inactivation in cultural heritage materials while minimizing the formation of radiation-induced optical defects. Samples CR2 and MZ were irradiated at room temperature (RT) at 25 °C, while CR1 and CR3 were processed under dry ice (DI) conditions placed inside a closed polystyrene container filled with solid CO_2 pellets, stabilizing the sample temperature at approximately −73 °C throughout irradiation. Dosimetry was performed using polymethyl methacrylate (PMMA) dosimeters positioned at the surface of each sample.

Microbiological analysis

Microbial contamination on the surface of the four glass plate negatives (CR1, CR2, CR3 and MZ) was quantified before and after irradiation using the contact-plate method. Fungal isolation from the samples was performed using sterile swabs moistened with sterile distilled water, which were rubbed across the entire surface of each photographic negative sample. Each swabs for each glass negative were then streaked in sterile Petri dishes (90 x 15 mm) containing dichloram-glycerol (DG18) agar medium (NEOGEN®, Lansing, MI, USA) plus 0.01% chloramphenicol (Pitt, Hocking, 2009) [26, 27]. DG18 agar is a selective medium used for counting and isolating xerophilic fungi in dry materials, such as glass negative samples [28].

After plating, the plates were incubated in a BOD (biochemical oxygen demand) incubator at 25 °C and relative humidity of 47% for 15 days. After 15 days, the plates were analyzed for the presence or absence of fungal growth and the colony formed units (CFU/surface). Surface contamination was quantified using Petri dishes with a 9-cm diameter (contact area = 63.6 cm^2). Colony-forming units per square centimeter (CFU/cm^2) were calculated by dividing the number of colonies observed after incubation by the effective sampling area. This unit is more appropriate for small rigid substrates such as 9 × 6.5 cm glass plate negatives, avoiding artificial extrapolation to 1 m^2 and providing a direct, comparable metric for before/after irradiation analyses. The different types of fungi were identified through morphological macroscopic and microscopic analysis. For macroscopic analysis, observe and reverse of the colonies, texture, size and coloration were observed. For microscopy, a fragment

of each fungal colony was placed between a slide and a coverslip, stained with lactophenol cotton blue, and observed under an optical microscope at 400x magnification.

The 6 kGy irradiated samples were divided into two groups: irradiated at room temperature (RT) and irradiated with dry ice (DI). The effectiveness of the decontamination process was evaluated by comparing microbial growth pre- and post-treatment.

Spectroscopy and colorimetric methods

All spectroscopic (UV–Vis) and colorimetric analyses were performed exclusively on the common glass samples (CG), which served as non-heritage analogues to systematically investigate radiation-induced optical effects. As previously explained, the historical photographic negatives could not be subjected to repeated spectroscopic measurements due to the sensitivity of their gelatin emulsions, the risk of mechanical stress during handling, and their irreplaceable nature.

UV-Vis spectrophotometry

To obtain the UV-Vis spectra, the equipment from the company Thermo Scientific, model Genesys 20, was used. The common glass samples were analyzed from a scan in the wavelength, in the range of 280–800 nm, to measure the absorption of ultraviolet and visible light by the samples and evaluate the changes in transparency and color.

Colorimetric measurements

Colorimetric analyses were conducted using a portable reflectance spectrophotometer PCE-CSM 8. The instrument operates with a 0°/45° measurement geometry, a spectral range from 400 to 700 nm, and uses the SQC8 color management system. This configuration is widely adopted in studies requiring objective quantification of perceptual color changes in transparent or semi-transparent materials. Color coordinates were obtained in the CIELAB 2000 system, which provides improved perceptual uniformity compared with the traditional CIELAB 1976 formulation [29, 30]. Total color difference (ΔE) between irradiated and unirradiated samples was calculated as Eq. 1.

$$\Delta E_{00} = \sqrt{\left(\frac{\Delta L\prime}{k_L S_L}\right)^2 + \left(\frac{\Delta C\prime}{k_C S_C}\right)^2 + \left(\frac{\Delta H\prime}{k_H S_H}\right)^2 + R_T\left(\frac{\Delta C\prime}{k_C S_C}\right)\left(\frac{\Delta H\prime}{k_H S_H}\right)} \quad (1)$$

where $\Delta L'$, $\Delta C'$, and $\Delta H'$ represent the differences in lightness, chroma, and hue, respectively; S_L, S_C, and S_H are the corresponding weighting functions for lightness, chroma, and hue; and k_L, k_C, and k_H denote the parametric constants associated with these same three components.

UVB bleaching procedures

For the bleaching treatment using light radiation, a UVB lamp from the brand NOMOY was selected, with an emission spectrum ranging from 280 to 320 nm and a power output of 26 watts. The gamma irradiated common glass samples (CG) were stored in light-protected packaging before being exposed to UVB light for 60 hours inside an expanded polystyrene box, and colorimeter readings were taken every 10 hours to obtain ΔE data. The gamma irradiated historical glass plate negatives (CR1, CR2, CR3 and MZ) were exposed for 20 hours inside an expanded polystyrene box. To more accurately assess the impact of the treatment on the images contained in the glass negatives, photographs were taken at 10-hour intervals during the exposure period using a Nikon D5100 digital single lens reflex (DSLR) camera equipped with a 55 mm lens. The images were converted to positive using GIMP 2.10, an open-source image editing software. The conversion process employed the 'Invert' and 'White Balance' tools, allowing for a more detailed analysis of the visual changes potentially caused by radiation processing.

Results and discussion

Elemental composition of glass substrates

Energy-dispersive X-ray spectroscopy (EDS) confirmed that all samples, CG, CR1, CR2, CR3 and MZ, correspond to soda–lime–silica (SLS) glass, composed mainly of Si, Na, Ca, Mg, and minor amounts of K and Fe (Table 1).

The additional components identified in the analysis, such as magnesium, aluminum, titanium, and potassium

Table 1 Commom glass (CG) and glass plate negative (CR1, CR2, CR3 and MZ) composition (wt%)

	Si	Na	Ca	Mg	Al	K	Fe	S	Ti	Zr	Cu	Sr	Ag	Mn
CG	74.650	10.686	7.188	3.450	3.378	0.195	0.177	0.199	0.050	0.008	0.007	0.004	–	–
CR1	74.338	8.217	9.569	3.462	2.763	0.208	0.182	0.277	0.053	0.010	0.007	0.003	0.047	–
CR2	75.156	8.824	8.640	3.401	3.322	0.144	0.120	0.214	0.063	0.010	0.004	0.004	0.085	0.013
CR3	72.314	8.295	15.921	–	2.534	0.158	0.334	0.303	0.094	0.008	0.006	0.009	0.023	–
MZ	79.161	6.112	8.070	2.827	2.964	0.417	0.111	0.164	0.045	0.010	0.006	0.004	0.098	0.012

contribute to the stability and durability of the glass, and zirconium is used in combination with titanium as nucleating agents [31, 32]. The detection of sulfur results from the use of sodium sulfate (Na_2SO_4) during the glass manufacturing process [14]. The iron detected in the samples can be considered an impurity derived from the mineral composition of sand [33, 34]. The presence of silver in photographic negative samples CR1, CR2, CR3, and MZ is consistent with the photographic development process, in which silver salts, the photosensitive components of the emulsion, are converted into metallic silver [35]. Samples CR2 and MZ containing manganese, commonly used historically as a decolorizing or refining additive of soda-lime glasses [36, 37] that can oxidize under irradiation, leading to purple coloration. The presence of Mn could be a significant variable in the interpretation of radiation-induced optical effects. Other minor amounts of impurities in the form of copper, strontium in the samples less than 1%.

Photographic emulsion identification

The type of photographic emulsion present on the glass plate negatives was identified using Fourier transform infrared absorption with attenuated total reflectance (FTIR-ATR). Figure 2 presents the FTIR-ATR spectra for the four photographic glass plate negative samples: CR1, CR2, CR3 and MZ.

FTIR-ATR analysis of the four historical glass plate negatives (CR1, CR2, CR3, and MZ) revealed characteristic bands associated with organic compounds, particularly within the 1700–1000 cm^{-1} region. Bands at approximately 1630 and 1530 cm^{-1} correspond to the amide I and amide II vibrations, respectively, and are consistent with the presence of gelatin, the primary binding material of the photographic emulsion in glass negatives [38–42]. Variations in band intensity among samples are attributed to differences in emulsion thickness, surface coverage, and the heterogeneous conservation state of the historical negatives, rather than to chemical degradation of the gelatin structure itself. Bands observed in the 2350–2400 cm^{-1} region are tentatively assigned to carbon dioxide-related absorptions or carbonate species. However, given their presence only in selected samples, these features may also be related to surface contamination or environmental residues rather than instrumental artifacts. Additionally, a broad band around 3300 cm^{-1} was observed and assigned to overlapping O–H (water) and N–H (amide) stretching vibrations, further supporting the presence of gelatin residues.

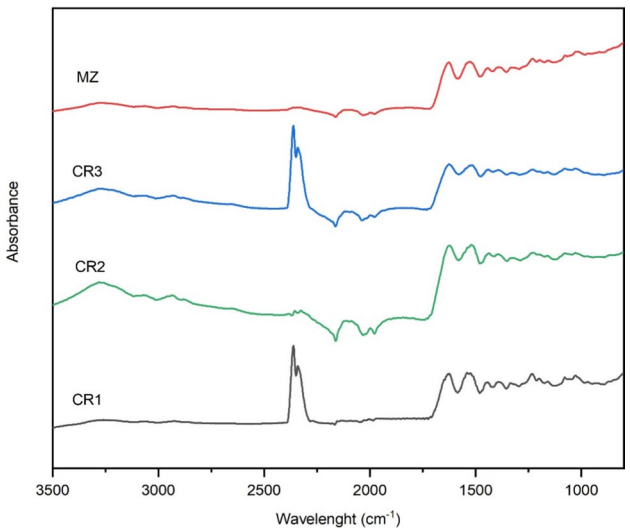

Fig. 2 FTIR-ATR spectra of glass plate negative samples

Radiation-induced optical changes in common glass samples

To investigate defect formation in glass-based materials of cultural heritage, controlled studies were conducted using the common glass samples (CG) irradiated at 2, 6, 10, 15 and 25 kGy at room temperature (RT) and with dry ice (DI), at a dose rate of 1 $kGy \cdot h^{-1}$.

UV–Vis absorbance

Due to the inherent transparency of glass, the control common glass samples (non-irradiated) exhibited UV–Vis spectra without absorption bands. Upon interaction with ionizing radiation, an increase in opacity and the development of an amber hue were observed, leading to the induction of two bands at 440 and 600 nm. These bands are associated with the activation of color centers and nonbridging oxygen hole centers (NBOHCs) in the glass samples [43–47]. Although the radiation-induced bands are broad, absorbance values at 440 and 600 nm were selected as representative points to enable consistent comparative analysis across doses and processing temperatures. These wavelengths correspond to maxima commonly associated with radiation-induced color centers in soda–lime silicate glass.

Figure 3 presents the UV–Vis spectra of the control (non-irradiated) and irradiated common glass samples at doses ranging from 2 to 25 kGy, both at room temperature (RT) and with dry ice (DI), immediately after each γ-ray irradiation. As the absorbed doses increased, the intensities of the bands at 440 nm and 600 nm also increased.

Table 2 presents the absorption values of the bands at 440 and 600 nm, obtained from the UV-vis spectra of the samples irradiated at different irradiation doses and in the two conditions of room temperature (RT) and with the use of dry ice (DI). The instrumental uncertainty provided by the manufacturer (±0.005 absorbance units) applies to all

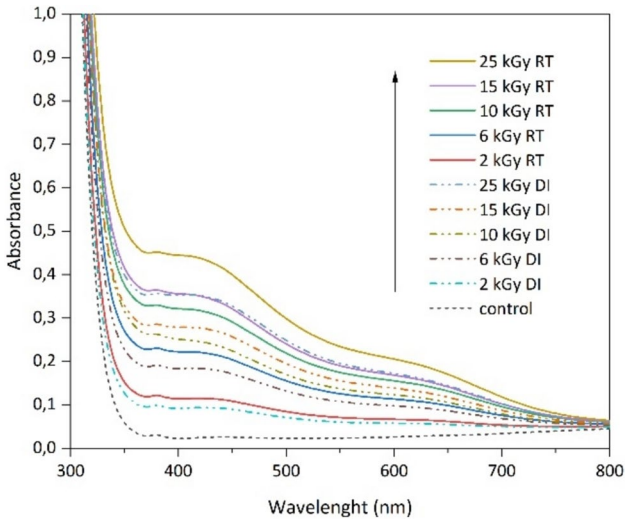

Fig. 3 UV-vis spectra of control and gamma-irradiated common glass samples, in RT (solid lines) and DI (dotted lines)

Table 2 Absorption values (Ae) at wavelengths of 440 and 600 nm of the irradiated samples at RT and DI

	440 nm		600 nm	
Dose (kGy)	RT	DI	RT	DI
Control	0.027	0.027	0.027	0.027
2	0.113	0.093	0.067	0.058
6	0.212	0.178	0.114	0.098
10	0.303	0.234	0.156	0.124
15	0.335	0.267	0.169	0.139
25	0.417	0.339	0.206	0.173

UV–Vis measurements and does not affect the comparative trends discussed in this study.

The use of dry ice during gamma ray irradiation resulted in lower absorption values compared with samples irradiated at room temperature. The protective effect of low temperatures can be attributed to the reduction in atomic and molecular mobility within the glass. At cold temperatures, the available energy for atomic and molecular movement decreases, reducing the probability of recombination or diffusion of crystalline defects induced by ionizing radiation [21, 48]. Furthermore, the formation and mobility of reactive species, such as free radicals, are restricted at lower temperatures [19]. Additionally, the cooling effect of dry ice further limits free radical propagation, reducing the formation of defects in the crystalline structure.

In order to evaluate the decay behavior of irradiation effects, the irradiated glass samples were stored in a dark environment to prevent interference from light radiation. Only the data at 440 nm are shown for clarity, as the absorbance behavior at 600 nm exhibited the same qualitative trend and did not provide additional information regarding the bleaching kinetics. Data were collected from the 440 nm band of UV-Vis spectra of samples after being irradiated for a period of 30 days.

Figure 4 illustrated the decay behavior of the specific absorption values at 440 nm in the UV-vis spectra of samples gamma irradiated at room temperature (RT) and with dry ice (DI), at doses ranging from 2 to 25 kGy.

The response curve shows an initial rapid decay within the first 24 hours, followed by a slower decay over the subsequent days, eventually reaching a plateau after 20 days. The observed fluctuations may be associated with the relaxation and recombination of radiation-induced electronic defects. The use of dry ice during irradiation resulted in lower

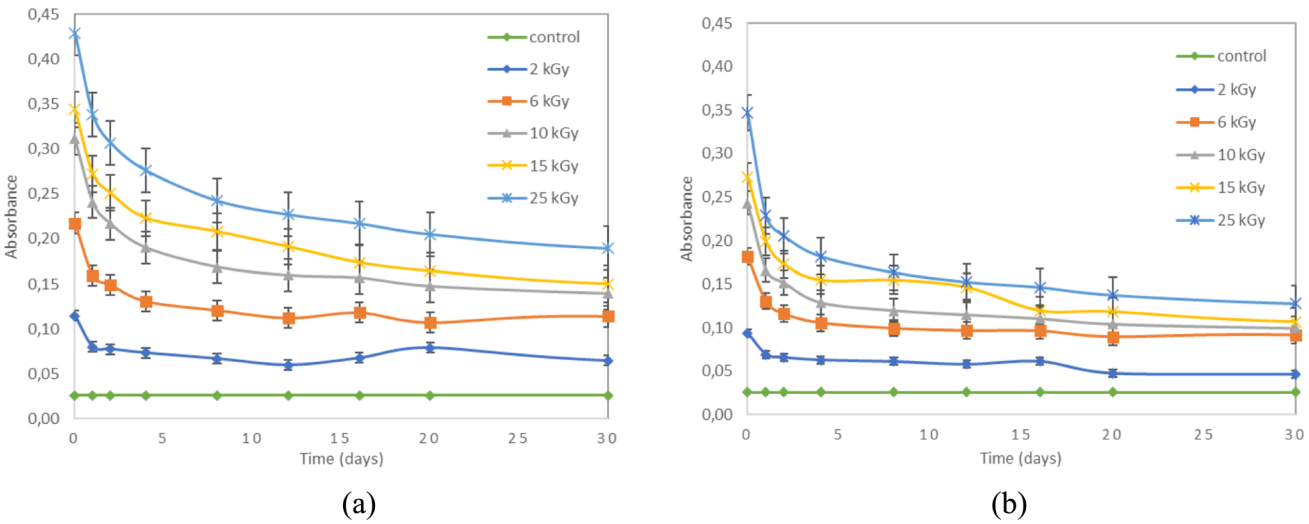

Fig. 4. 440 nm band absorption induced by gamma rays in common glass samples at RT (**a**) and DI (**b**), until 30 days

absorption values at 440 nm throughout the entire 30-day period. This trend is more pronounced at higher absorbed doses, whereas at lower doses (up to 6 kGy) the recovery kinetics for RT and DI samples are comparable within experimental uncertainty. The findings of this study align with previous research by Ezz-Eldin et al. [33] and Madbouly et al. [49], which demonstrated that irradiation-induced NBOHC defects are unstable at room temperature, leading to the gradual decay of increased optical density over time.

Colorimetric changes

The total color difference index, expressed as ΔE, is the primary parameter used to evaluate and quantify whether the colorimetric changes observed in the irradiated samples are perceptible to the naked eye. Table 3 presents the ΔE values as a function of the absorbed doses for gamma irradiation, recorded on the 1st and 30th days, comparing the thermal processing conditions at room temperature (RT) and under dry-ice cooling (DI) at doses ranging from 2 to 25 kGy. The uncertainty associated with colorimetric measurements was ±0.2 ΔE units, according to the instrument specifications.

To interpret the ΔE values obtained for the irradiated samples, the classification criteria proposed by Hardeberg [50] were adopted: ΔE values below 3 are considered minimally perceptible to the human eye and therefore generally do not represent a significant impact on the visual appearance of the material. Values between 3 and 6 are classified as perceptible but acceptable, indicating that although a chromatic change occurs, it remains tolerable within conservation contexts. Values above 6 are considered unacceptable, as they reflect clear and potentially compromising visual alterations affecting the aesthetic and documentary integrity of the object. Based on this classification, it is possible to evaluate the visual impact of ionizing radiation on the irradiated glass samples.

For the gamma-irradiated samples, ΔE values exceeded the threshold of 6 even at the lowest tested dose of 2 kGy. Under RT conditions, the ΔE value was 9.023, while under DI conditions it was 7.56. These values fall within the "unacceptable" range and increased progressively with dose up to the maximum of 25 kGy. Samples irradiated at low temperature exhibited lower values compared to those irradiated at room temperature, confirming the protective effect of low temperatures during processing. The results indicated that after 30 days, some degree of transparency recovery was observed, particularly in samples irradiated with dry ice, which appeared lighter compared to their immediately irradiated state. However, transparency remained affected, and an amber hue was still present. Based on the ΔE values obtained, irradiation at disinfection doses starting from 6 kGy resulted in ΔE values exceeding 6 after 30 days, indicating unacceptable color changes in the glass. This suggests the need for complementary strategies to mitigate darkening and restore the optical transparency of the irradiated material.

The observed impacts on transparency and the persistence of the brownish tone after the analyzed period are consistent with the studies of Ruller and Friebele [51] and Kadono et al. [16], which suggest that ionizing-induced coloration can stabilize due to electron trapping in hydrogen atoms generated by the radiolysis during irradiation.

Table 3 Total color difference (ΔE) values of common glass samples irradiated at room temperature (RT) and with dry ice (DI), calculated on the 1st and 30th days after processing, at doses of 2 to 25 kGy

	RT		DI	
Dose (kGy)	Day 1	Day 30	Day 1	Day 30
2	9.023	4.898	7.558	4.140
6	18.519	10.604	14.863	8.540
10	26.104	15.435	18.845	10.947
15	30.024	17.333	22.472	12.614
25	35.542	21.217	25.615	14.618

UVB bleaching performance

Exposure of common glass samples (CG) to controlled UVB irradiation demonstrated partial reversibility of the radiation-induced color centers. Table 4 presents colorimetric readings were performed at 10-hour intervals throughout the exposure period. Colorimetric values at 0 h correspond to measurements performed within 24 hours after irradiation and prior to UVB exposure.

The results indicate that optimal UVB exposure time depends on the absorbed dose. For samples irradiated at 2 kGy, significant recovery occurred within 10 h, whereas higher doses required longer exposure times. Therefore, UVB bleaching should be applied in a controlled, stepwise manner with periodic visual and colorimetric assessment. Notably, when UVB radiation was applied to samples processed with dry ice (DI), time required to restore transparency was reduced when compared to samples irradiated at room temperature (RT). This short exposure time is advantageous, as it minimizes prolonged interaction of the vitreous material with light radiation, potentially reducing the risk of additional damage. Low-temperature irradiation acts as a preventive strategy by reducing the formation and stabilization of radiation-induced color centers. UVB exposure, in contrast, functions as a post-irradiation remedial treatment, partially reversing residual optical alterations when they occur.

The radiation emitted by the UVB lamp provided sufficient energy to break the bonds that caused the electronic

Table 4 ΔE values every 10 hours up to a limit of 60 hours in response to UVB lamp exposure at room temperature (RT) and dry ice (DI) for samples of common glass gamma irradiated in different doses. Colorimetric measurements present an instrumental uncertainty of ±0.2 ΔE units

	2 kGy		6 kGy		10 kGy		15 kGy		25 kGy	
Exposure hours	RT	DI	RT	DI	RT	DI	RT	DI	RT	DI
0	10.828	9.096	22.556	18.045	27.752	19.981	33.296	24.972	36.459	26.250
10	4.172	3.505	10.696	8.557	13.613	9.801	17.692	13.269	19.270	13.875
20	2.743	2.305	7.415	5.932	9.630	6.934	11.324	8.493	12.990	9.353
30	2.072	1.740	5.269	4.215	6.890	4.961	8.545	6.409	10.355	7.456
40	1.609	1.352	4.225	3.380	5.492	3.954	7.140	5.355	7.495	5.397
50	1.430	1.201	3.767	3.014	4.855	3.495	5.356	4.017	6.650	4.788
60	1.206	1.013	3.027	2.422	4.007	2.885	4.726	3.545	5.346	3.849

defects in the vitreous lattice [52]. As a result, the energy from the UVB radiation was able to release the trapped electrons and recombine them with NBOHCs, promoting the restoration of transparency to the glass [16].

The results obtained in this study demonstrated that exposure to a UVB lamp is an effective procedure for restoring the transparency of irradiated glass, being an alternative to the heat treatment traditionally used for brightening these materials. Furthermore, the UVB lamp has the advantage of not causing heating that could lead to alterations in the structure of the photographic emulsion, which is sensitive to higher temperatures, making it a safe option for application to photographic negatives on glass plates.

Microbiological analysis of historical glass plate negatives

The glass plate photographic negative samples exhibited significant microbial growth, confirming active contamination before irradiation. After macroscopic analysis of the cultured plates for the four glass negative samples, fungal growth was observed in all samples. Microscopy allowed the identification of fungi based on the observation of their reproductive structures, revealing the presence of genera such as *Aspergillus* spp., *Cladosporium* spp. and *Penicillium* spp. Nine isolates that did not present reproductive structures, were subcultured in sterile Petri dishes (60 × 15 mm) and incubated at 25 °C and 47% relative humidity for 7 days. Even under these conditions, which are suitable for the growth and sporulation of xerophilic and storage-related fungi, no reproductive structures were observed. Therefore, these isolates were considered non-sporulating fungi (NSF). Table 5 presents the total count in colony forming units (CFU) per surface (63.6 cm^2 contact area), pre- and post-irradiation, as well as the identification of the fungi isolated from the samples.

Before irradiation, all samples exhibit microbial loads. Although numerically low, these values represent active fungal contamination when expressed over the 63.6 cm^2 contact area of the Petri dishes. After exposure to 6 kGy gamma radiation, no microbial growth was observed on any plate, confirming complete inactivation under both room temperature and dry-ice conditions.

Table 6 presents the culture plates before and after processing with ionizing radiation. Samples CR2 and MZ were irradiated at room temperature (RT), whereas samples CR1 and CR3 were processed under low temperature (DI). After irradiation, all samples presented zero CFU counts, confirming the efficacy of the treatment at an absorbed dose of 6 kGy, even under low temperature conditions during processing. Thus, all samples irradiated at 6 kGy (RT and DI) showed a complete reduction in fungal growth,

Table 5 Counting in CFU per surface and identification of fungi isolated from samples

Sample	Dose (kGy)	Temperature during irradiation (°C)	Pre-irradiation (CFU/cm^2)	Identification morphology	Post-irradiation (CFU/cm^2)
CR1	6	−73	0.03	1 *Cladosporium* spp. 1 NSF*	0.00
CR2	6	25	0.05	2 *Cladosporium* spp. 1 NSF*	0.00
CR3	6	−73	0.18	6 *Cladosporium* spp. 2 *Penicillium* spp. 4 NSF*	0.00
MZ	6	25	0.06	1 *Penicillium* spp. 3 NSF*	0.00

*non-sporulating fungus

Table 6 Images of plates cultures pre- and post-irradiation (6kGy) of glass plate negatives CR1, CR2, CR3 and MZ processed with both temperature variation (RT and DI)

	CR1/DI	CR2/RT	CR3/DI	MZ/RT
Pre-irradiation				
Post-irradiation				

demonstrating the effectiveness of gamma radiation for decontamination.

These results are fully consistent with the well-established fungicidal window of 6–8 kGy recommended for cultural heritage materials and confirm that temperature does not influence microbial inactivation.

Visual impact of gamma irradiation on image quality

The four samples were previously subjected to gamma irradiation: negatives CR2 and MZ were irradiated at room temperature (RT), while CR1 and CR3 were irradiated under dry ice conditions (DI). A dose of 6 kGy was selected as it corresponds to the lower end of the internationally recommended 8 ± 2 kGy window for effective fungal inactivation in heritage materials, thereby reducing the likelihood of generating pronounced radiation-induced color or transparency changes. Table 7 presents images of the glass negative samples before and after gamma irradiation.

The interaction with ionizing radiation predominantly breaks Si–O–Si bonds, releasing electrons and generating intrinsic defects such as E′ centers (≡Si•) and non-bridging oxygen hole centers, NBOHCs (≡Si–O•). These defects are responsible for strong absorption in the visible region, resulting in a characteristic brownish tone of the samples. These defects may form independently or jointly, and additional electrons can become trapped at modifier-related sites (Na^+, Ca^{2+}, Fe^{3+}, Al^{3+}), contributing to induce optical density increase [44, 53–55]. As a result, a noticeable darkening of the glass negatives was observed after irradiation, consistent with the expected effects of applied dose.

Table 7 Glass plate negative samples before and after irradiation with an absorbed dose of 6 kGy

	CR1/DI	CR2/RT	CR3/DI	MZ/RT
Pre-irradiation				
Post-irradiation				

UVB light exposure of gamma irradiated glass plate negatives

For the historical glass plate photographic negatives, UVB exposure was applied cautiously, with measurements and visual inspections at 5-hour intervals to avoid exposing gelatin emulsions to excessive photonic flux.

The results of UVB light exposure of gamma irradiated glass plate negatives are presented in Table 8. The negative images were digitally converted into positive images to visually assess the impact on the photographic content of the effects of ionizing radiation and subsequent exposure to UVB light. This approach is essential for assessing the preservation of visual information, which is critical not only for conservators and restorers of photographic materials but also for ensuring continued public access to these historical records. In the positive images, a slight loss of contrast was observed in the irradiated samples. After exposure to UVB light, a gradual recovery of contrast and image sharpness was noted in all samples. This progressive improvement observed during UVB exposure confirmed its beneficial role in bringing the images closer to their original pre-irradiation appearance.

No clear visual differences were observed between samples processed at room temperature and under dry ice conditions. This outcome is likely influenced by intrinsic variations in the composition and tonal range of the photographic images themselves. In addition, the apparent difficulty in visually distinguishing differences between samples is partly due to the low absorbed dose applied to the historical negatives (6 kGy), intentionally selected at the lower limit of the recommended fungicidal window to minimize optical alteration. Under these conditions, radiation-induced changes are subtle and predominantly manifest as slight contrast variations rather than pronounced visible discoloration.

Although irradiation at room temperature represents is a viable option when low-temperature processing is not feasible, cooling with dry ice is recommended for collections in which preservation of both aesthetic and structural integrity is crucial. Low-temperature irradiation mitigates the formation and

Table 8 Positive images of samples irradiated with 6 kGy during periods of exposure to UVB radiation

Hours post-irradiation	CR1/DI	CR2/RT	CR3/DI	MZ/RT
Control				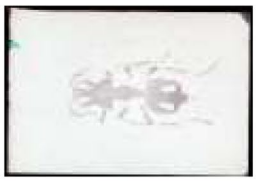
0				
10				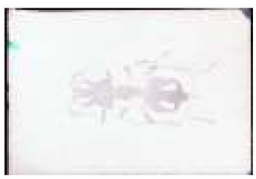
20				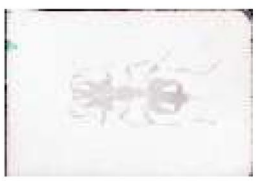

stabilization of radiation-induced optical defects in the glass matrix by reducing atomic and electronic mobility. However, this preventive effect does not completely suppress optical darkening, particularly at doses within the fungicidal range. In this context, subsequent UVB exposure acts as a corrective post-treatment, attenuating residual color alterations and improving image legibility. Therefore, low-temperature irradiation and UVB bleaching should be regarded as complementary strategies rather than mutually exclusive approaches. Cooling the samples also contributes to the preservation of the photographic emulsion, which is highly sensitive to heat and prone to softening, swelling, or partial denaturation during thermal fluctuations. Maintaining the emulsion at low temperature during irradiation helps preserve its mechanical stability and reduces the risk of deformation or separation from the glass substrate. The transition from room temperature to approximately −73 °C is safe for soda–lime–silica glass when performed gradually and without direct contact between the glass and the dry ice. Under these controlled conditions, no thermal shock, cracking, or delamination was observed. Therefore, low-temperature irradiation provides an effective safeguard against optical and physical degradation for both the glass matrix and the photographic emulsion. In this way, the combined strategy of low temperature irradiation followed by UVB exposure is a suitable alternative for heritage institutions seeking to balance the biocidal effect with long-term conservation of materials.

The results indicate that there is no single optimal UVB bleaching time that can be universally applied to glass plate photographic negatives. The effectiveness of UVB exposure is strongly dependent on the absorbed radiation dose and on the extent of radiation-induced optical alteration in the glass support. Lower doses at the lower limit of the recommended fungicidal range ensure biocidal effectiveness while inducing less pronounced color alterations in the glass plates, thereby requiring shorter UVB exposure times to improve visual appearance. For historical glass plate negatives, UVB exposure was applied conservatively, with periodic visual inspections at short time intervals to avoid unnecessary light stress on the photographic emulsion. Under these conditions, exposure times up to 20 hours proved sufficient to improve image legibility without inducing additional damage. Therefore, UVB bleaching should be regarded as a controlled, dose-dependent post-treatment, in which exposure time must be adjusted according to the irradiation history and the visual response of each object, rather than as a fixed protocol.

Conclusions

The study found that ionizing radiation processing with a dose of 6 kGy was effective in completely eliminating fungal contamination from photographic negatives on glass plates, both at room temperature and with the use of dry ice. Microbiological analysis demonstrated that lowering the temperature to −73 °C during processing did not compromise disinfection efficacy, indicating that the radiosensitivity of microorganisms was preserved under low temperature conditions. In addition, dry ice cooling during irradiation helped reduce the extent of radiation-induced color center formation, thereby limiting initial optical alterations in the glass support.

Nevertheless, low-temperature processing alone does not completely prevent optical darkening. Post-irradiation exposure to UVB light proved to be an effective non-thermal strategy for attenuating residual color changes and improving image legibility. The bleaching efficiency was dependent on the absorbed dose, indicating that no single UVB exposure time is universally applicable.

Therefore, the combination of low-temperature irradiation as a preventive measure and UVB exposure as a corrective post-treatment constitutes a balanced and adaptable methodology for the conservation of glass-based photographic heritage materials.

Acknowledgements The authors acknowledge the support of Nuclear and Energy Research Institute (IPEN-CNEN/SP), Institute of Biomedical Sciences (ICB-USP) and Museum of Ethnology and Archeology (MAE-USP) of the University of São Paulo.

Author Contributions All authors contributed to the study conception and design. Material preparation, data collection and analysis were performed by Maria Luiza Emi Nagai, Elizabeth S. R. Somessari, Tatiana A. Reis, and Pablo A. S. Vasquez. The first draft of the manuscript was written by Maria Luiza Emi Nagai and all authors commented on previous versions of the manuscript. All authors read and approved the final manuscript.

Funding The Article Processing Charge (APC) for the publication of this research was funded by the Coordenação de Aperfeiçoamento de Pessoal de Nível Superior - Brasil (CAPES) (ROR identifier: 00x0ma614).

Declarations

Conflict of interest The authors declare that they have no known competing financial interests or personal relationships that could have appeared to influence the work reported in this paper.

Open Access This article is licensed under a Creative Commons Attribution 4.0 International License, which permits use, sharing, adaptation, distribution and reproduction in any medium or format, as long as you give appropriate credit to the original author(s) and the source, provide a link to the Creative Commons licence, and indicate if changes were made. The images or other third party material in this article are included in the article's Creative Commons licence, unless indicated otherwise in a credit line to the material. If material is not included in the article's Creative Commons licence and your intended use is not permitted by statutory regulation or exceeds the permitted use, you will need to obtain permission directly from the copyright holder. To view a copy of this licence, visit http://creativecommons.org/licenses/by/4.0/.

References

1. Valverde M (2005) Photographic negatives: nature and evolution of processes. Image Permanence Institute, New York
2. Kwiatkowska M, Ważny R, Turnau K, Wójcik A (2016) Fungi as deterioration agents of historic glass plate negatives of Brandys family collection. Int Biodeterior Biodegrad 115:133–140. https://doi.org/10.1016/j.ibiod.2016.08.002
3. Conides CA (2015) Preserving and accessing the Howard D. Beach photography studio glass plate negative collection. Collect A J Museum Arch Prof 11:83–101. https://doi.org/10.1177/155019061501100202
4. Kosel J, Ropret P (2021) Overview of fungal isolates on heritage collections of photographic materials and their biological potency. J Cult Herit 48:277–291. https://doi.org/10.1016/j.culher.2021.01.004
5. Marušić K, Klarić MŠ, Sinčić L et al (2020) Combined effects of gamma-irradiation, dose rate and mycobiota activity on cultural heritage – study on model paper. Radiat Phys Chem 170:108641. https://doi.org/10.1016/j.radphyschem.2019.108641
6. Cortella L, Albino C, Tran QK, Froment K (2020) 50 years of French experience in using gamma rays as a tool for cultural heritage remedial conservation. Radiat Phys Chem 171:108726. https://doi.org/10.1016/j.radphyschem.2020.108726
7. Vadrucci M, De Bellis G, Mazzuca C et al (2020) Effects of the ionizing radiation disinfection treatment on historical leather. Front Mater 7:1–9. https://doi.org/10.3389/fmats.2020.00021
8. Nagai ML, Santos P, Parron I et al (2022) Gamma radiation processing for disinfection of a 19th century photo album. Braz J Radiat Sci 10:1–6. https://doi.org/10.15392/2319-0612.2022.2008
9. International Atomic Energy Agency (2017) Uses of ionizing radiation for tangible cultural heritage conservation. IAEA, Vienna
10. de Oliveira LN, do Nascimento EO, Andreeta MRB et al (2019) Characterization of lithium diborate, sodium diborate and commercial soda-lime glass exposed to gamma radiation via linearity analyses. Radiat Phys Chem 155:133–137. https://doi.org/10.1016/j.radphyschem.2018.06.031
11. Farah K, Kovács A, Mejri A, Ben Ouada H (2007) Effect of post-irradiation thermal treatments on the stability of gamma-irradiated glass dosimeter. Radiat Phys Chem 76:1523–1526. https://doi.org/10.1016/j.radphyschem.2007.02.065
12. Sendova M, Jim A, Crawford CL (2023) In situ optical microspectroscopy study of isothermal bleaching of γ-irradiated International Simple Glass. ACS Phys Chem Lett. https://doi.org/10.1021/acsphyschemau.3c00020
13. Borgman VA (2006) Kinetics of photoinduced recombination of hole-type color centers in silicate glasses. Glas Phys Chem 32:280–286. https://doi.org/10.1134/S1087659606030047
14. Abd-Allah R (2022) From decolorization to solarization of historical glass: a review. Adv Res Conserv Sci 3:30–41. https://doi.org/10.21608/arcs.2022.135911.1025
15. Jiang L, Sheng J (2005) Solarization of silver-doped soda-lime silicate glass containing X-ray induced color centers. J Mater Sci 9:5177–5180. https://doi.org/10.1007/s10853-005-4410-5
16. Kadono K, Itakura N, Akai T et al (2009) Effect of additive ions on the optical density and stability of the color centers induced by X-ray irradiation in soda-lime silicate glass. Nucl Instrum Methods Phys Res Sect B: Beam Interact Mater At 267:2411–2415. https://doi.org/10.1016/j.nimb.2009.04.014
17. Craven E, Hasanain F, Winters M (2012) Minimizing material damage using low temperature irradiation. Radiat Phys Chem 81:1254–1258. https://doi.org/10.1016/j.radphyschem.2012.01.013
18. Burton B, Gaspar A, Josey D et al (2014) Bone embrittlement and collagen modifications due to high-dose gamma-irradiation sterilization. Bone 61:71–81. https://doi.org/10.1016/j.bone.2014.01.006
19. Jastrzebska A, Kaminski A, Grazka E et al (2014) Effect of gamma radiation and accelerated electron beam on stable paramagnetic centers induction in bone mineral: influence of dose, irradiation temperature and bone defatting. Cell Tissue Bank 15:413–428. https://doi.org/10.1007/s10561-013-9406-9
20. Fernández-Carballido A, Puebla P, Herrero-Vanrell R, Pastoriza P (2006) Radiosterilisation of indomethacin PLGA/PEG-derivative microspheres: protective effects of low temperature during gamma-irradiation. Int J Pharm 313:129–135. https://doi.org/10.1016/j.ijpharm.2006.01.034
21. Ramalingam S, Samsuddin SM, Yusof N et al (2018) Performance of cooling materials and their composites in maintaining freezing temperature during irradiation and transportation of bone allografts. J Orthop Surg 26:1–8. https://doi.org/10.1177/2309499018770906
22. Kaminski A, Jastrzebska A, Grazka E et al (2012) Effect of gamma irradiation on mechanical properties of human cortical bone: Influence of different processing methods. Cell Tissue Bank 13:363–374. https://doi.org/10.1007/s10561-012-93082
23. International Atomic Energy Agency (2008) Trends in Radiation Sterilization of Health Care Products. Vienna
24. Ponta CC (2017) Emergency intervention at National Film Archive. In: Uses of Ionizing Radiation for Tangible Cultural Heritage Conservation. Vienna, pp 131–135
25. Area MC, Calvo AM, Felissia FE et al (2014) Influence of dose and dose rate on the physical properties of commercial papers commonly used in libraries and archives. Radiat Phys Chem 96:217–222. https://doi.org/10.1016/j.radphyschem.2013.10.004
26. Purkrtova S, Savicka D, Kadava J et al (2022) Microbial Contamination of Photographic and Cinematographic Materials in Archival Funds in the Czech Republic. Microorganisms 10:1–20. https://doi.org/10.3390/microorganisms10010155
27. Sclocchi MC, Kraková L, Pinzari F et al (2017) Microbial life and death in a foxing stain: a suggested mechanism of photographic prints defacement. Microb Ecol 73:815–826. https://doi.org/10.1007/s00248-016-0913-7
28. Corry JEL, Curtis GDW, Baird RM (2003) Dichloran glycerol (DG18) agar. In: Corry JEL, Curtis GDW, Baird RM (eds) Handbook of culture media for food microbiology. Elsevier, pp 453–455
29. Chmielewska-Śmietanko D, Gryczka U, Migdał W, Kopeć K (2018) Electron beam for preservation of biodeteriorated cultural heritage paper-based objects. Radiat Phys Chem. https://doi.org/10.1016/j.radphyschem.2017.07.008
30. Sharma G, Wu W, Dalal EN (2005) The CIEDE2000 color-difference formula: implementation notes, supplementary test data, and mathematical observations. Color Res Appl 30:21–30. https://doi.org/10.1002/col.20070
31. da Luz AB, Lins FAF (2008) Areia Industrial. Rochas e Minerais Industriais: usos e especificações. CETEM/MCT, Rio de Janeiro, pp 167–186
32. Mandal K, Ghose S, Mandal M et al (2021) Notes on useful materials and synthesis through various chemical solution techniques. Elsevier Inc, Amsterdam
33. Ezz-Eldin FM, Mahmoud HH, Abd-Elaziz TD, El-Alaily NA (2008) Response of commercial window glass to gamma doses. Phys B Condens Matter 403:576–585. https://doi.org/10.1016/j.physb.2007.09.074
34. Kadono K, Itakura N, Akai T et al (2010) Effects of iron on the formation and annihilation of X-ray irradiation induced non-bridging oxygen hole centers in soda-lime silicate glass. J Non-Cryst Solids 356:232–235. https://doi.org/10.1016/j.jnoncrysol.2009.11.013

35. Short NM, Malin D, Light DL (2007) The focal encyclopedia of photography. Elsevier, Oxford
36. El-Badry KM, Abo-Naf SM, Saad EA et al (2010) Efficiency of decolorizing agents in the production of colorless commercial glasses from municipal glass cullet wastes. Glass Phys Chem 36:190–198. https://doi.org/10.1134/S1087659610020070
37. Nassau K (2003) The Physics and chemistry of color: The 15 mechanisms. In: The Science of Color. Optical Society of America, Elsevier, pp 247–280
38. Noohi S, Dehkordi MH (2025) Causes of silver mirroring and yellowing on a nineteenth-century photographic gelatin glass plate negative. Stud Conserv 0:1–9. https://doi.org/10.1080/00393630.2024.2448929
39. Oravec M, Haberová K, Jančovičová V et al (2019) Identification of the historic photographic print materials using portable NIR and PCA. Microchem J 150:104202. https://doi.org/10.1016/j.microc.2019.104202
40. Zachariášová B, Haberová K, Oravec M, Jančovičová V (2019) Plasma treatment of gelatin photography. Acta Chim Slov 12:27–33. https://doi.org/10.2478/acs-2019-0005
41. Tomšová K, Ďurovič M, Drábková K (2016) The effect of disinfection methods on the stability of photographic gelatin. Polym Degrad Stab 129:1–6. https://doi.org/10.1016/j.polymdegradstab.2016.03.034
42. Mišková L, Hudec R, Novák P, Novotná M (2016) Astronomical glass plate negatives: monitoring of emulsion layer deterioration. Acta Polytech 56:57–61. https://doi.org/10.14311/APP.2016.56.0057
43. Wang J, Cheng J, Shao C et al (2024) Effects of oxygen loading on the red-luminescence of non-bridging oxygen hole centers in γ -irradiated silica glasses. Opt Mater 147:114707. https://doi.org/10.1016/j.optmat.2023.114707
44. Kadono K, Itakura N, Akai T et al (2010) Formation of color centers in a soda-lime silicate glass by excimer laser irradiation. J Phys Condens Matter. https://doi.org/10.1088/0953-8984/22/4/045901
45. Natura U, Ehrt D (1999) Formation of radiation defects in silicate and borosilicate glasses caused by UV lamp and excimer laser irradiation. Glas Sci Technol -Frankfurt am Main 72:295–301
46. Sheng J, Kadono K, Utagawa Y, Yazawa T (2002) X-ray irradiation on the soda-lime container glass. Appl Radiat Isot 56:621–626. https://doi.org/10.1016/S0969-8043(01)00238-X
47. Vanina EA, Chibisova MA, Sokolova SM (2006) Effect of radiation bleaching in sodium-silicate glasses. Glas Ceram (English Transl Steklo i Keramika) 63:366–367. https://doi.org/10.1007/s10717-006-0124-7
48. Walo M, Przybytniak G, Nowicki A, Awieszkowski W (2011) Radiation-induced effects in gamma-irradiated PLLA and PCL at ambient and dry ice temperatures. J Appl Polym Sci 122:375–383. https://doi.org/10.1002/app.34079
49. Madbouly AM, Alazab HA, Borham E, Ezz-ElDin FM (2021) Study of gamma radiation dosimeter and radiation shielding parameters of commercial window glass. Appl Phys A Mater Sci Process 127:1–14. https://doi.org/10.1007/s00339-021-04889-9
50. Gerhardt J, Hardeberg JY (2008) Spectral color reproduction minimizing spectral and perceptual color differences. Color Res Appl 33:494–504. https://doi.org/10.1002/col.20444
51. Ruller JA, Friebele EJ (1991) The effect of gamma-irradiation on the density of various types of silica. J Non-Cryst Solids 136:163–172. https://doi.org/10.1016/0022-3093(91)90131-O
52. Wang Z, Qian L, Peng X et al (2021) New aspects of degradation in silicone rubber under uva and uvb irradiation: A gas chromatography–mass spectrometry study. Polymers (Basel) 13:1–12. https://doi.org/10.3390/polym13132215
53. Messina F (2007) Role of hydrogen on the generation and decay of point defects in amorphous silica exposed to UV laser radiation. Universtià degli Studi di Palermo
54. Agnello S, Gelardi FM, Boscaino R et al (2002) Intrinsic defects induced by β-irradiation in silica. Nucl Instr Methods Phys Res Sect B Beam Interact Mater At 191:387–391. https://doi.org/10.1016/S0168-583X(02)00546-3
55. Abd MAOWM, Sallam AOI (2022) Gamma ray interaction with soda lime silicate glasses doped with V 2 O 5, CuO or SrO. Appl Phys A 128:1–12. https://doi.org/10.1007/s00339-022-05522-z

Publisher's Note Springer Nature remains neutral with regard to jurisdictional claims in published maps and institutional affiliations.